Numerical Study of Mixed Convection Heat Transfer in Methanol based Micropolar Nanofluid about a Horizontal Circular Cylinder

Numerical Study of Mixed Convection Heat Transfer in Methanol based Micropolar Nanofluid about a Horizontal Circular Cylinder

M Z Swalmeh[1,2], H T Alkasasbeh[2], A Hussanan[4,5]* and M Mamat[1]

[1] Faculty of Informatics and Computing, Universiti Sultan Zainal Abidin (Kampus Gong Badak), 21300 Kuala Terengganu, Terengganu, Malaysia
[2] Faculty of Arts and Sciences, Aqaba University of Technology, Aqaba-Jordan
[3] Department of Mathematics, Faculty of Science, Ajloun National University, P.O. Box 43, Ajloun 26810, Jordan
[4]Division of Computational Mathematics and Engineering, Institute for Computational Science, Ton Duc Thang University, Ho Chi Minh City, Vietnam
[5]Faculty of Mathematics and Statistics, Ton Duc Thang University, Ho Chi Minh City, Vietnam

* Email: abidhussanan@tdtu.edu.vn

Abstract. In this article, the mixed convection boundary layer flow about a horizontal circular cylinder with a micropolar nanofluid, which is maintained at a constant surface heat flux, has been investigated. Three types of nanoparticles with distinct conductivities, namely, graphene oxide, copper and copper oxide are considered and suspended in methanol based micropolar nanofluid. The governing equations are transformed into nonlinear PDEs by applying the similarity transformations and then solved numerically by an implicit finite difference scheme known as Keller-box method. The results for the local wall temperature, local skin friction coefficient, temperature, velocity and angular velocity are plotted and discussed for different parameters such as nanoparticles volume fraction and mixed convection parameter in view of thermo-physical properties of nanoparticles and base fluid. Moreover, numerical results for the local wall temperature and local skin friction coefficient are obtained. It is found that copper (Cu) suspended methanol based micropolar nanofluid have higher velocity than the copper oxide (CuO) or graphene oxide (GO) methanol based micropolar nanofluid. Comparison have been made with published results on Newtonian fluid under special cases and obtained in close agreement.

1. Introduction

A nanofluid is comprised of suspended solid nanoparticles in the convectional base fluids having size with a size smaller than 100 nm [1]. Such fluids have better thermophysical properties than the convectional fluids. The commonly used materials for nanoparticles made of chemically stable metals (Au, Cu, Al, Ag, Fe), oxides ceramics (CuO, Al2O3, TiO2, SiO2), nonmetals (single and multi-walls carbon nanotubes, graphite) and functionalized nanoparticles. These nanoparticles enhance the thermal conductivity and convective heat transfer coefficient of base fluid significantly. Buongiorno [2]

published an article on the convective transport in nanofluids. Tiwari and Das [3] investigated numerically the heat transfer augmentation in a two sided lid-driven differentially heated square cavity utilizing copper–water nanofluid. The nanofluids used to acquire optimum thermal properties at the lowest volume fraction of nanoparticles in the base fluid by Godson et al. [4]. Kandelousi [5] also considered the nanofluid flow and heat transfer through a permeable channel. Entropy generation analysis for MHD nanofluid flow over rotating disk was carried out by Rashidi et al. [6]. Malvandi and Ganji [7] examined the onset of magnetic force on nanoparticles migration and heat transfer of water/alumina nanofluid in a channel. Haq et al. [8] studied the slip effect on heat transfer nanofluid flow past a stretching surface. Zhang et al. [9] examined the power law flow of a nanofluid thin film past a linearly stretched surface with slip velocity and variable magnetic field. Hussanan et al. [10] described the characteristics of carbon nanotubes-water nanofluid past stretching sheet with Newtonian heating. Few recent attempts on nanofluids can be found in [11-17].

The classical Navier-Stokes theory described the flow properties of Newtonian and non-Newtonian materials, but this theory was not suitable to describe micro-rotations, certain microscopic effects growing from the local structure of fluid elements and some naturally arising fluids, which are known as micropolar or thermomicropolar fluids. Micropolar fluid theory and its dilation to thermomicropolar fluids were initially introduced by Eringen [18]. Further, many physicists, engineers and mathematicians have been studied on the micropolar fluid to conclude the different results related to flow problems. Hassanien et al. [19] considered boundary layer heat transfer flow of micropolar fluid over stretching. Papautsky et al. [20] investigated the laminar micropolar fluid flow in microchannels. Hussanan et al. [21] explained the unsteady natural convection flow of a micropolar fluid on a vertical plate oscillating in its plane with Newtonian heating condition. Natural convection through a micropolar fluid heat and mass transfer flow over a vertical plate was analyzed by Hussanan et al. [22] utilizing Newtonian heating condition. Free convection boundary layer flow of micropolar fluid on a solid sphere with convective boundary conditions was considered by Alkasasbeh et al. [23]. Alkasasbeh [24] explores the heat transfer magnetohydrodynamic flow of micropolar Casson fluid on a horizontal circular cylinder with thermal radiation. Natural convection on boundary layer flow of Cu-water and Al_2O_3-water micropolar nanofluid about a solid sphere investigated by Swalmeh et al. [25]. Micropolar forced convection flow over moving surface under magnetic field was investigated by Waqas et al. [26].

The heat transfer through a boundary layer in the mixed convection flow about a circular cylinder has a vast space in applied technology, such as solving the cooling problems in turbine blades, boiler design, hotwire anemometry, conductor's electronic systems and manufacturing processes. The heat transfer over a isothermal horizontal isothermal cylinder with natural-convection is investigated by Kuehn et al. [27]. Recent articles in the direction of boundary layer flow for an isothermal circular cylider can be stated [28-30]

The aim of this paper is to study the mixed convection boundary layer flow over a horizontal circular cylinder in a micropolar nanofluid with constant heat flux. The graphene oxide (GO), copper (Cu) and copper oxide (CuO) suspended in methanol-based micropolar nanofluid. The boundary layer equations are solved numerically via efficient implicit finite-difference scheme known as the Keller-box method, as displayed by [31]. The effects of the nanoparticle volume fraction parameters, the mixed convection and micro-rotation parameter on the local heat transfer, local skin friction, temperature, velocity and angular velocity around the circular cylinder are discussed and explained in the tables and figures. For comparison purposes, the present results for regular Newtonian fluid are computed, and they show excellent agreement with those obtained by [32].

2. Basic Equations

Consider the steady laminar two-dimensional incompressible boundary layer flow of a micropolar nanofluid past a horizontal cylinder, with uniform free stream $(1/2)U_\infty$. Figure 1 explains the flow model and physical coordinate system, the free stream temperature T_∞, $\bar{x}-\bar{y}$ orthogonal coordinates

along the surface of the cylinder, q_w the constant heat flux with $(q_w > 0)\,\lambda > 0$ for an assisting flow and $(q_w < 0)\,\lambda < 0$ for an opposing flow, and *a* the radius of the horizontal cylinder.

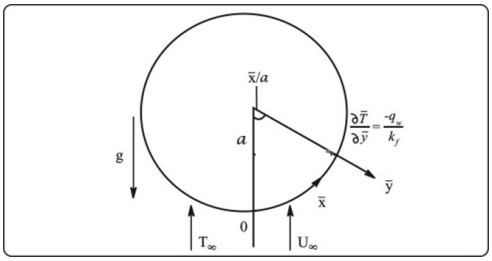

Figure 1. Physical model and coordinate system.

Under Boussinesq and boundary layer approximations, the governing equation 1 – 4 can be written as:

$$\frac{\partial \bar{u}}{\partial \bar{x}} + \frac{\partial \bar{v}}{\partial \bar{y}} = 0, \tag{1}$$

$$\begin{aligned} \bar{u}\frac{\partial \bar{u}}{\partial \bar{x}} + \bar{v}\frac{\partial \bar{u}}{\partial \bar{y}} &= \bar{u}_e \frac{d\bar{u}_e}{d\bar{x}} + \left(\frac{\mu_{nf} + \kappa}{\rho_{nf}}\right)\frac{\partial^2 \bar{u}}{\partial \bar{y}^2} + \frac{\kappa}{\rho_{nf}}\frac{\partial \bar{H}}{\partial \bar{y}}, \\ &+ \frac{\left(\chi\rho_s\beta_s + (1-\chi)\rho_f\beta_f\right)}{\rho_{nf}} g\left(T - T_\infty\right)\sin\left(\frac{\bar{x}}{a}\right) \end{aligned} \tag{2}$$

$$\rho_{nf} j\left(\bar{u}\frac{\partial \bar{H}}{\partial \bar{x}} + \bar{v}\frac{\partial \bar{H}}{\partial \bar{y}}\right) = -\kappa\left(2\bar{H} + \frac{\partial \bar{u}}{\partial \bar{y}}\right) + \phi_{nf}\frac{\partial^2 \bar{H}}{\partial \bar{y}^2}, \tag{3}$$

$$\bar{u}\frac{\partial T}{\partial \bar{x}} + \bar{v}\frac{\partial T}{\partial \bar{y}} = \alpha_{nf}\frac{\partial^2 T}{\partial \bar{y}^2}, \tag{4}$$

where

$$\begin{aligned} &\alpha_{nf} = \frac{k_{nf}}{(\rho C_p)_{nf}},\ \rho_{nf} = (1-\chi)\rho_f + \chi\rho_s,\ \mu_{nf} = \frac{\mu_f}{(1-\chi)^{2.5}}, \\ &(\rho C_p)_{nf} = (1-\chi)(\rho C_p)_f + \chi(\rho C_p)_s,\ \phi_{nf} = \left(\mu_{nf} + \kappa/2\right) j, \\ &\frac{k_{nf}}{k_f} = \frac{(k_s + 2k_f) - 2\chi(k_f - k_s)}{(k_s + 2k_f) + \chi(k_f - k_s)}, \end{aligned} \tag{5}$$

which are defined by [25]. Here χ is the nanoparticles volume fraction. In a special case, when $\chi = 0$ represents classical micropolar fluid. Further, α_{nf} is the thermal diffusivity of the nanofluid, μ_{nf} is the viscosity of the nanofluid, ϕ_{nf} is the spin gradient viscosity of the nanofluid , $(\rho C_p)_{nf}$ is the heat capacity of the nanofluid, j is micro-inertia density and all other symbols and quantities are given in nomenclature. Using the boundary conditions suitable for the system corresponding equation 1 – 5 [32]

$$\begin{aligned} &\bar{u} = \bar{v} = 0,\ \frac{\partial T}{\partial \bar{y}} = \frac{-q_w}{k_{nf}}\ ,\ \ \bar{H} = -\frac{1}{2}\frac{\partial \bar{u}}{\partial \bar{y}}\ \text{as}\ \bar{y} = 0, \\ &\bar{u} \to \bar{u}_e(\bar{x}),\ T \to T_\infty\ \ H \to 0\ \ \text{as}\ \bar{y} \to \infty, \end{aligned} \tag{6}$$

we consider that $\overline{u}_e(\overline{x}) = U_\infty \sin\left(\overline{x}/a\right)$ is the local free-stream velocity, here $\overline{u}$ and $\overline{v}$ are the velocity components along the $\overline{x}-\overline{y}$ plane, respectively. $\overline{H}$ is the microrotation components normal to $\overline{x}-\overline{y}$ plane. Now, we introduce the following non-dimensional variables:

$$x = \frac{\overline{x}}{a},\ \ y = \mathrm{Re}^{2/5}\left(\frac{\overline{y}}{a}\right),\ r(x) = \frac{\overline{r}(\overline{x})}{a},\ \theta = \mathrm{Re}^{2/5}\left(\frac{T-T_\infty}{aq_w/k}\right),$$
$$u = \frac{\overline{u}}{U_\infty},\ \ v = \mathrm{Re}^{2/5}\left(\frac{\overline{v}}{U_\infty}\right),\ v = \mathrm{Re}^{2/5}\left(\frac{\overline{v}}{U_\infty}\right),\ \ H = \left(\frac{a}{U_\infty}\right)\mathrm{Re}^{-2/5}\,\overline{H}, \tag{7}$$

where $\mathrm{Re} = U_\infty\, a/v_f$ is the Reynolds number and v_f is the kinematic viscosity of the fluid. Substituting the previous variables into equation 1 – 4, we obtain the following boundary-layer equations for the problem under dimensionless form

$$\frac{\partial u}{\partial x} + \frac{\partial u}{\partial y} = 0, \tag{8}$$

$$u\frac{\partial u}{\partial x} + v\frac{\partial u}{\partial y} = u_e\frac{\partial u_e}{\partial x} + \frac{\rho_f}{\rho_{nf}}\left(D(\chi)+K\right)\frac{\partial^2 u}{\partial y^2} + \frac{1}{\rho_{nf}}\left(\chi\rho_s\left(\frac{\beta_s}{\beta_f}\right)+(1-\chi)\rho_f\right)\lambda\theta\sin x + \frac{\rho_f}{\rho_{nf}}K\frac{\partial H}{\partial y}, \tag{9}$$

$$u\frac{\partial\theta}{\partial x} + v\frac{\partial\theta}{\partial y} = \frac{1}{\mathrm{Pr}}\left[\frac{k_{nf}/k_f}{(1-\chi)+\chi\left(\rho c_p\right)_s/\left(\rho c_p\right)_f}\right]\frac{\partial^2\theta}{\partial y^2}, \tag{10}$$

$$u\frac{\partial H}{\partial x} + v\frac{\partial H}{\partial y} = -\frac{\rho_f}{\rho_{nf}}K\left(2\overline{H} + \frac{\partial\overline{u}}{\partial\overline{y}}\right) + \frac{\rho_f}{\rho_{nf}}\left(D(\chi)+\frac{K}{2}\right)\frac{\partial^2 H}{\partial y^2}, \tag{11}$$

where $D(\chi) = 1/(1-\chi)^{2.5}$, $K = \kappa/\mu_f$ is the micropolar parameter, $\mathrm{Pr} = v_f/\alpha_f$ is the Prandtl number and the mixed convection parameter λ, which is defined as $\lambda = Gr/\mathrm{Re}^{5/2}$ with $Gr = g\beta_f\left(aq_w/k\right)\left(a^3/v_f^2\right)$ is the Grashof number for constant surface heat flux boundary conditions. It is important mentioning that $\lambda > 0$ for an assisting flow ($T_w > T_\infty$) (heated flow), $\lambda < 0$ for an opposing flow ($T_w < T_\infty$) (cooled flow) and $\lambda = 0$ the forced convection flow. The boundary conditions (5) become:

$$u = v = 0,\ \ \frac{\partial\theta}{\partial y} = -1,\ \ H = -\frac{1}{2}\frac{\partial u}{\partial y}\ \text{ as }\ y = 0,$$
$$u \to u_e(x) = \frac{\sin x}{x},\ u \to 0,\ \ \theta \to 0,\ \ H \to 0\ \text{ as }\ y \to \infty. \tag{12}$$

We assume the following variables to solve equation 8 – 11, subject to boundary conditions (12)

$$\psi = xf(x.y),\ \theta = \theta(x,y),\ H = xh(x,y), \tag{13}$$

where ψ is the stream function defined as $u=\partial\psi/\partial y$ and $v=-\partial\psi/\partial x$, which satisfies the continuity equation 8. Substituting the equation 13 into 9 to 11, we obtain the following transformed equations:

$$\frac{\rho_f}{\rho_{nf}}\left(D(\chi)+K\right)\frac{\partial^3 f}{\partial y^3}+f\frac{\partial^2 f}{\partial y^2}-\left(\frac{\partial f}{\partial y}\right)^2+\frac{1}{\rho_{nf}}\left(\chi\rho_s\left(\frac{\beta_s}{\beta_f}\right)+(1-\chi)\rho_f\right)\lambda\frac{\sin x}{x}\theta$$
$$+\frac{\sin x\cos x}{x}+\frac{\rho_f}{\rho_{nf}}K\frac{\partial h}{\partial y}=x\left(\frac{\partial f}{\partial y}\frac{\partial^2 f}{\partial x\partial y}-\frac{\partial f}{\partial x}\frac{\partial^2 f}{\partial y^2}\right), \tag{14}$$

$$\frac{1}{\Pr}\left[\frac{k_{nf}/k_f}{(1-\chi)+\chi(\rho c_p)_s/(\rho c_p)_f}\right]\frac{\partial^2\theta}{\partial y^2}+f\frac{\partial\theta}{\partial y}=x\left(\frac{\partial f}{\partial y}\frac{\partial\theta}{\partial x}-\frac{\partial f}{\partial x}\frac{\partial\theta}{\partial y}\right), \tag{15}$$

$$\frac{\rho_f}{\rho_{nf}}\left(D(\chi)+\frac{K}{2}\right)\frac{\partial^2 h}{\partial y^2}+f\frac{\partial h}{\partial y}-\frac{\partial f}{\partial y}h-\frac{\rho_f}{\rho_{nf}}K\left(2h+\frac{\partial^2 f}{\partial y^2}\right)=x\left(\frac{\partial f}{\partial y}\frac{\partial h}{\partial x}-\frac{\partial f}{\partial x}\frac{\partial h}{\partial y}\right), \tag{16}$$

The boundary conditions (12) become:

$$f=\frac{\partial f}{\partial y}=0,\ \theta'=-1,\ h=-\frac{1}{2}\frac{\partial^2 f}{\partial y^2}\ \text{as}\ y=0,$$
$$\frac{\partial f}{\partial y}\to\frac{\sin x}{x}\ \ \theta\to 0,\ h\to 0\ \text{as}\ y\to\infty. \tag{17}$$

In practical application, the physical quantities of interest are the local skin friction coefficient C_f and local wall temperature θ_w which is written in non-dimensional form as

$$C_f=\left(D(\chi)+\frac{K}{2}\right)x\frac{\partial^2 f}{\partial y^2}(x,0),\ \ \theta_w=\theta(x,0). \tag{18}$$

3. Results and Discussion

The governing equations 14 – 16 subject to the boundary conditions (17) have been solved numerically using Keller-box method, along with Newton's linearization technique as described by [31] and plotted for different values of parameters for skin friction coefficient, local wall temperature, temperature, velocity and angular velocity fields, at different positions x for the assisting $(\lambda>0)$ and opposing $(\lambda<0)$ flow. We have used data related to thermo-physical properties of the fluid and nanoparticles as given in table 1. The comparison of the local skin friction coefficient at $K=0$ and $\chi=0$ (regular Newtonian fluid) compared with [32] presented in table 2 and to satisfy the accuracy of the present method. We have found the wall temperature and local skin friction are in a good agreement.

Table 1. Thermo-physical properties of based fluids and nanoparticle.

Physical properties	methanol	Cu	CuO	GO
ρ (kg/m^3)	792	8933	6320	1800
C_p (J/kg – K)	2545	385	531.8	717
K (W/m – K)	0.2035	400	76.5	5000
$\beta\times10^{-5}(K^{-1})$	149	1.67	1.80	28.4
Pr	7.38			…..

Table 2. Values of local skin friction coefficient C_f for $K = 0$ and $\chi = 0$ (Newtonian fluid), Pr=1, and various values of λ ([32]).

x	λ								
	-0.85	-0.6	-0.4	-0.2	0.0	0.2	0.34	0.35	5.0
0°	0.0000	0.0000	0.0000	0.0000	0.0000	0.0000	0.0000	0.0000	0.0000
	(0.0000)	(0.0000)	(0.0000)	(0.0000)	(0.0000)	(0.0000)	(0.0000)	(0.0000)	(0.0000)
0.2	0.0034	0.1027	0.1586	0.2035	0.2424	0.2777	0.3005	0.30215	0.79379
	(0.0170)	(0.0917)	(0.1547)	(0.2020)	(0.2421)	(0.2778)	(0.3009)	(0.3025)	(0.7947)
0.4		0.1739	0.2918	0.3837	0.4619	0.5331	0.5789	0.58214	1.5592
		(0.1456)	(0.2816)	(0.3788)	(0.4600)	(0.5319)	(0.5783)	(0.5815)	(1.5595)
0.6		0.1263	0.3755	0.51900	0.6377	0.7465	0.8154	0.8202	2.2700
		(0.1051)	(0.3550)	(0.5084)	(0.6331)	(0.7422)	(0.8121)	(0.8170)	(2.2683)
0.8			0.3817	0.5916	0.7526	0.9017	0.9941	1.0005	2.9035
			(0.3475)	(0.5721)	(0.7447)	(0.8926)	(0.9866)	(0.9931)	(2.8983)
1.0			0.2291	0.5868	0.7946	0.9884	1.1048	1.1128	3.4409
			(0.2097)	(0.5537)	(0.7827)	(0.9725)	(1.0912)	(1.0993)	(3.4311)
1.2				0.4917	0.7570	1.0009	1.1430	1.1527	3.8689
				(0.4360)	(0.7410)	(0.9773)	(1.1218)	(1.1316)	(3.8535)
1.4				0.2007	0.6377	0.9453	1.1116	1.1229	4.1667
				(0.1585)	(0.6175)	(0.9094)	(1.0811)	(1.0927)	(4.1575)
1.6					0.4345	0.8276	1.0144	1.0332	4.3685
					(0.4095)	(0.7774)	(0.9786)	(0.9920)	(4.3397)
1.8					0.09641	0.6648	0.8774	0.89946	4.4363
					(0.0408)	(0.5955)	(0.8296)	(0.8448)	(4.002)
2.0						0.4611	0.7274	0.74331	4.3852
						(0.3817)	(0.6544)	(0.6713)	(4.3411)
2.2						0.2510	0.5747	0.59145	4.2175
						(0.1565)	(0.4765)	(0.4950)	(4.1643)
2.4							0.4607	0.4726	3.9337
							(0.3212)	(0.3404)	(3.8695)
2.6							0.4317	0.4390	3.5290
							(0.2107)	(0.2282)	(3.4503)
2.8							0.5078	0.5206	2.9885
							(0.1488)	(0.1614)	(2.8888)
3.0								0.6682	2.2733
								(0.1078)	(2.1391)
π								0.7886	1.5001
								(0.0303)	(1.4046)

The demeanors of the local skin friction coefficient C_f and the wall temperature θ_w for the copper, copper oxide and graphene oxide in methanol with the effect of different parameters, such as nanoparticle volume fraction χ, with different values of *x,* are shown in the figure 2 and 3. From these figures, it is noticed that the local wall temperature and the local skin friction coefficient show the same trend for variations in the nanoparticle volume fraction. The local wall temperature and the local skin friction coefficient exhibited increasing behavior for increasing values of χ, for a longer time. It is also detected that Cu has higher local wall temperature than CuO/GO, but GO has higher local skin friction compared CuO/Cu, when the nanoparticles density increase, for various value of χ.

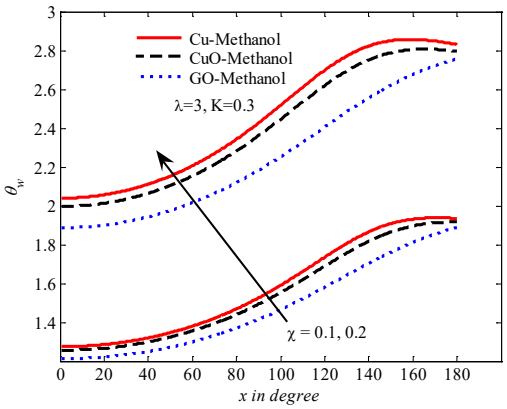

Figure 2. Comparison of the local wall for various values of x and χ.

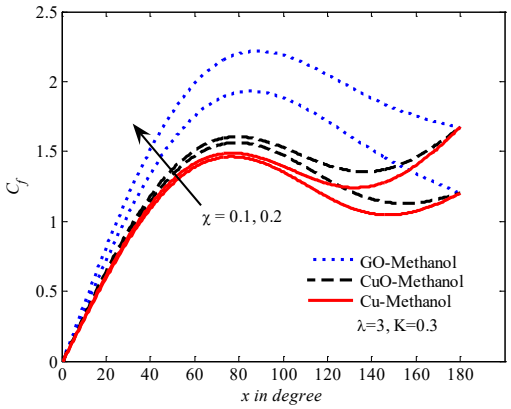

Figure 3. Comparison of the local skin friction for various values of x and χ.

The influence of the mixed convection parameter on the local wall temperature and the local skin friction is studied in figure 4 and 5. The trends of local wall temperature and the local skin friction, are opposite to each other. the local wall temperature decreases with increasing λ, but the local skin friction increase. Further, the local wall temperature θ_w of GO methanol is higher than CuO/Cu when ($\lambda < 0$) (cooled cylinder). Besides that, the opposite happens when ($\lambda > 0$) (heated cylinder), GO methanol is lower local wall temperature θ_w than CuO/Cu. On the other hand, the local skin friction of GO is higher than CuO/Cu methanol when $(\lambda > 0)$ (heated cylinder), but when $(\lambda < 0)$ (cooled cylinder), GO methanol is lower local wall temperature θ_w than CuO/Cu, this is because of the physical properties for nanoparticles.

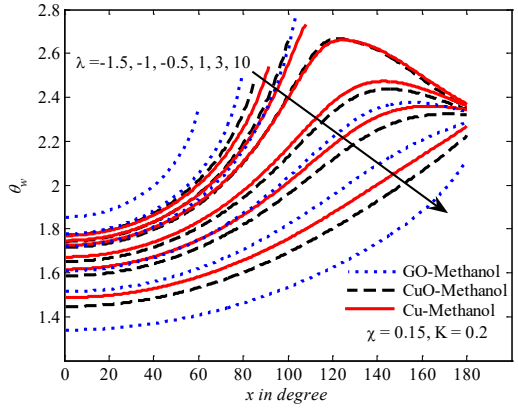

Figure 4. Comparison of the local wall temperature for various values of x and λ.

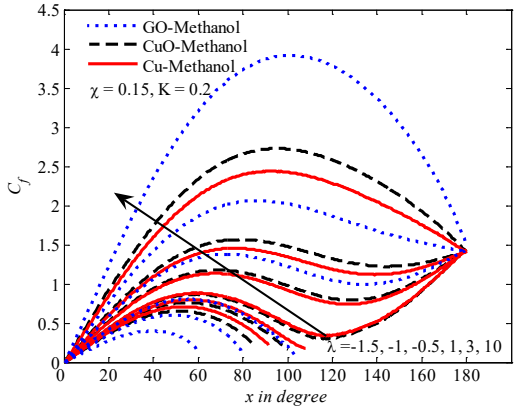

Figure 5. Comparison of the local skin for various values of x and λ.

Figure 6 and 7 display the velocity and the angular velocity profiles at the lower stagnation point of the circular cylinder $x \approx 0$ of the copper, copper oxide and graphene oxide, suspended in based fluid namely methanol, for the nanoparticle volume fraction χ. From these figures, it is found that velocity and the angular velocity profiles increase with increasing values of nanoparticle volume fraction χ. It can be observed that from figure 8 to 9 the temperature field increases as increase χ. Further, Cu methanol has a higher temperature compared with CuO/GO based nanofluids. Furthermore, we found that the Cu methanol has a higher temperature as compared to CuO/GO based nanofluids, when the

mixed convection parameter λ increases as shown in figure 9. It is also observed that there is a sharp rise in temperature with the increase of mixed convection parameter λ.

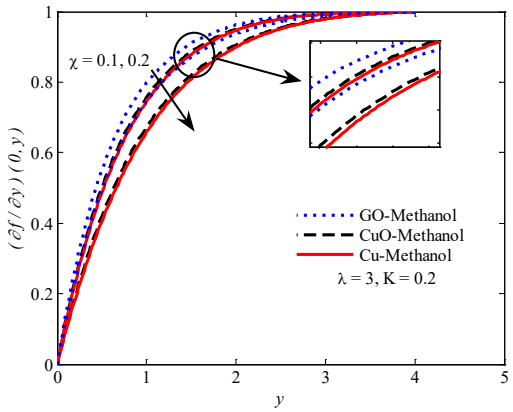

Figure 6. Velocity profiles at $x \approx 0$ for various values of χ.

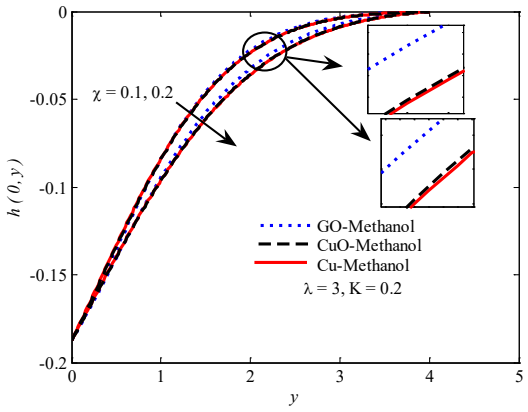

Figure 7. Angular velocity profiles at $x \approx 0$ for various values of χ.

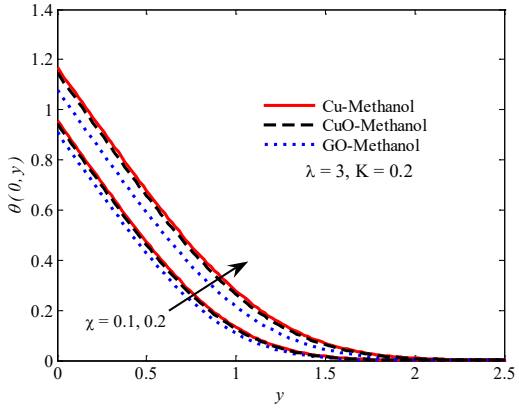

Figure 8. Temperature profiles at $x \approx 0$ for various values of χ.

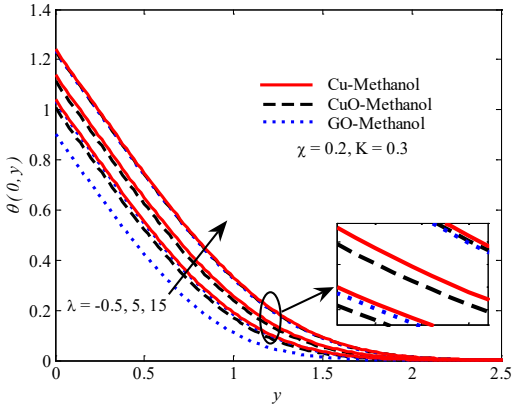

Figure 9. Temperature profiles at $x \approx 0$ for various values of λ.

In the last figure 10 and 11, the velocity and angular velocity has the same behaviours for the nanoparticles that GO methanol has lower velocity and angular velocity when ($\lambda < 0$) (cooled cylinder), but when ($\lambda > 0$) (heated cylinder), GO methanol has higher velocity and angular velocity compared with CuO/GO methanol based micropolar nanofluid.

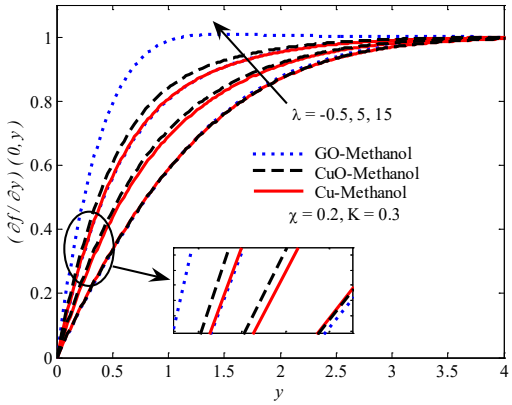

Figure 10. Velocity profiles at $x \approx 0$ for various values of λ.

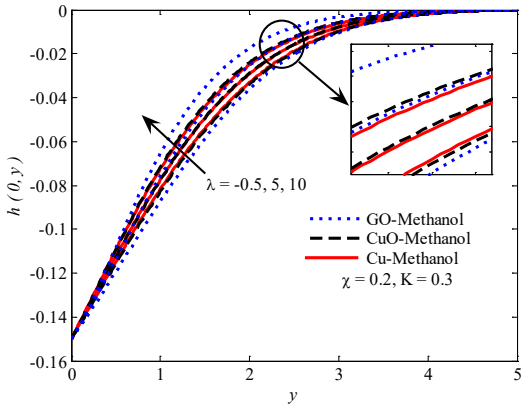

Figure 11. Angular velocity profiles at $x \approx 0$ for various values of λ.

4. Conclusions

In this study, the mixed convection flow of three different types of nanoparticles such as copper, copper oxide and graphene oxide suspended in methanol based micropolar nanofluid over a horizontal circular cylinder with constant heat flux is investigated. The problem is modelled and then solved via Keller box method. Results were plotted and discussed. The following major points were concluded.

i. Cu has a higher than CuO/GO-methanol based micropolar nanofluid in local wall temperature and temperature profiles but noticed adverse influences in the case of local skin friction for GO-methanol with increasing nanoparticle volume, micro-rotation parameter and mixed convection parameter $(\lambda > 0)$.

ii. The temperature, velocity and angular velocity increase with an increase in mixed convection parameter. However the velocity and angular velocity decrease with an increase in nanoparticle volume and micro-rotation parameter.

iii. GO has a higher velocity and angular velocity compared with CuO/Cu-methanol based micropolar nanofluid for different values of nanoparticle volume, micro-rotation parameter and mixed convection parameter $(\lambda > 0)$.

Nomenclature

$C_{p,nf}$	Nanofluid heat capacity $\left[J \cdot kg^{-1} \cdot K^{-1}\right]$
g	Acceleration due to gravity $\left[m \cdot s^{-2}\right]$
Gr	Grashof number
j	Micro-inertia density $\left[m^2\right]$
K	Micro-rotation parameter
k_f	Base fluid thermal conductivity $\left[W \cdot m^{-1} \cdot K^{-1}\right]$
k_s	Solid particles thermal conductivity $\left[W \cdot m^{-1} \cdot K^{-1}\right]$
k_{nf}	Nanofluid thermal conductivity $\left[W \cdot m^{-1} \cdot K^{-1}\right]$
$\bar{H}$	Angular velocity $\left[m \cdot s^{-1}\right]$
Pr	Prandtl number

T Temperature of the fluid $\left[K\right]$

T_w Wall temperature $\left[K\right]$

T_∞ Ambient temperature $\left[K\right]$

u x-component of velocity $\left[m \cdot s^{-1}\right]$

v y-component of velocity $\left[m \cdot s^{-1}\right]$

Greek symbols

α_{nf} Nanofluid thermal diffusivity $\left[m^2 \cdot s^{-1}\right]$

χ Nanoparticles volume fraction

κ Vortex viscosity $\left[kg \cdot m^{-1} \cdot s^{-1}\right]$

μ_f Base fluid dynamic viscosity $\left[kg \cdot m^{-1} \cdot s^{-1}\right]$

μ_{nf} Nanofluid dynamic viscosity $\left[kg \cdot m^{-1} \cdot s^{-1}\right]$

ρ_f Base fluid density $\left[kg \cdot m^{-3}\right]$

ρ_s Solid particles density $\left[kg \cdot m^{-3}\right]$

ρ_{nf} Nanofluid density $\left[kg \cdot m^{-3}\right]$

β_f Base fluid thermal expansion coefficient $\left[K^{-1}\right]$

β_s Solid particles thermal expansion coefficient $\left[K^{-1}\right]$

ϕ_{nf} Spin gradient viscosity $\left[kg \cdot m \cdot s^{-1}\right]$

ψ Stream function

θ Dimensionless temperature

Subscripts

w Condition at wall

∞ Condition at infinity

References

[1] Choi S U S. 1995 *ASME: Fluids Engineering Division*; **231**: 99.
[2] Buongiorno J. 2006 *J.heat trans.*; **128**: 240.
[3] Tiwari R K and Das M K. 2007 *Inte. J.Heat and Mass Trans.*; **50**: 2002.
[4] Godson L, Raja B, Lal D M and Wongwises S. 2010 *Renble sustable energy revws*; **14**: 629.
[5] Kandelousi M S. 2014 *Phys Letts A*; **378**: 3331.
[6] Rashidi M M, Abelman S and Mehr N F. 2013 *Int. J. Heat Mass Transfer*; **62**: 515.
[7] Malvandi A and Ganji D D. 2014 *J. Magn. Magn. Mater.*; **362**: 172.
[8] Haq R U, Nadeem S, Khan Z H and Noor N. 2015 *Phys B: cond.matt.*; **457**: 40.
[9] ZhangY, Zhang and Bai Y. 2017 *J. Taiwan Inst. Chem. Eng.*; **70**: 104.
[10] Hussanan A, Khan I, Gorji MR and Khan WA. 2019 *BioNanoScience*; https://doi.org/10.1007/s12668-018-0592-6
[11] Oztop H F and Abu-Nada E. 2008 *Int. j.heat and fluid flow*; **29**: 1326.
[12] Das S K, Choi S U and Patel H E. 2006 *Heat trans eng*; **27**: 3.
[13] Kandelousi M S. 2014 *The Eur.Phys. J. Plus*; **129**: 248.
[14] Qasim M, Khan Z, Lopez R and Khan W. 2016 *The Eur. Phys. J. Plus*; **131**: 16.

[15] Hussanan A, Khan I, Hashim H, Mohamed M K A, Ishak N, Sarif N M and Salleh M Z. 2016 *J. Teknologi*; **78**.
[16] Tlili I, Khan W and Khan I. 2018 *Results in physics*; **8**: 213.
[17] Alkasasbeh H T, Swalmeh M Z, Hussanan A and Mamat M. 2019 CDF lett; 1.
[18] Eringen AC. 1966 *J.Mathematics and Mechanics*: 1.
[19] Hassanien I, Abdullah A and Gorla R. 1998 *Applied Mechanics and Engineering*; **3**: 377.
[20] Papautsky I, Brazzle J, Ameel T and Frazier A B. 1999 *Sens. actuat. A: Phys.*; **73**: 101.
[21] Hussanan A, Salleh M Z, Khan I and Tahar R M. 2017 *Thermal Science*; **21**: 2313.
[22] Hussanan A, Salleh M Z, Khan I and Tahar R M. 2018 *Neural Comp. Appl.*; **29**: 59.
[23] Alkasasbeh H T, Salleh M Z, Tahar R M, Nazar R and Pop I. 2014 *W. Appl. Scie. J.*; **32**: 1942.
[24] Alkasasbeh H. 2018 *Frontiers in Heat and Mass Transfer (FHMT)*; **10**.
[25] Swalmeh M Z, Alkasasbeh H T, Hussanan A and Mamat M. 2018 *Res. Phys.*; **9**: 717.
[26] Waqas H, Hussain S, Sharif H and Khalid S. 2017 *Br. J. Math. Comput. Sci.*; **21**: 1.
[27] Saitoh T, Sajiki T and Maruhara K. 1993 *Int. J. of Heat and Mass Trans.*; **36**: 1251.
[28] Morgan V T. 1975.; *Adv. in heat trans.*;11: 199.
[29] Sparrow E and Lee L. 1976 *Int. J. of Heat and Mass Trans.*; **19**: 229.
[30] Nazar R, Amin N and Pop I. 2003 *Int. J. Num. Meth. Heat & Fluid. Flow*; **13**: 86.
[31] Cebeci T and Bradshaw P. Spr. Science & Business Media; 2012.
[32] Nazar R, Amin N and Pop I. 2004 *Heat and mass transfer*; **40**: 219.